THE JOURNAL OF BIOLOGICAL CHEMISTRY VOL. 291, NO. 32, pp. 16424–16437, August 5, 2016

The Endocytic Fate of the Transferrin Receptor Is Regulated by c-Abl Kinase*[S]

Received for publication, March 3, 2016, and in revised form, May 24, 2016 Published, JBC Papers in Press, May 24, 2016, DOI 10.1074/jbc.M116.724997

Hong Cao[‡], Barbara Schroeder[§1], Jing Chen[‡], Micah B. Schott[‡], and Mark A. McNiven[‡2]

From the [‡]Department of Biochemistry and Molecular Biology, Center for Basic Research in Digestive Diseases, and [§]Department of Experimental Pathology and Laboratory Medicine, Mayo Clinic, Rochester, Minnesota 55905

Clathrin-mediated endocytosis of transferrin (Tf) and its cognate receptor (TfR1) is a central pathway supporting the uptake of trophic iron. It has generally been assumed that this is a constitutive process. However, we have reported that the non-receptor tyrosine kinase, Src, is activated by Tf to facilitate the internalization of the Tf-TfR1 ligand-receptor complex. As an extension of these findings, we have tested whether subsequent trafficking steps might be regulated by additional kinase-dependent cascades, and we observed a significant endocytic block by inhibiting c-Abl kinase by a variety of methods. Importantly, Tf internalization was reduced significantly in all of these cell models and could be restored by re-expression of WT c-Abl. Surprisingly, this attenuated Tf-TfR1 endocytosis was due to a substantial drop in both the surface and total cellular receptor levels. Additional studies with the LDL receptor showed a similar effect. Surprisingly, immunofluorescence microscopy of imatinib-treated cells revealed a marked colocalization of internalized TfR1 with late endosomes/lysosomes, whereas attenuating the lysosome function with several inhibitors reduced this receptor loss. Importantly, inhibition of c-Abl resulted in a striking redistribution of the chaperone Hsc70 from a diffuse cytosolic localization to an association with the TfR1 at the late endosome-lysosome. Pharmacological inhibition of Hsc70 ATPase activity in cultured cells by the drug VER155008 prevents this chaperone-receptor interaction, resulting in an accumulation of the TfR1 in the early endosome. Thus, inhibition of c-Abl minimizes receptor recycling pathways and results in chaperone-dependent trafficking of the TfR1 to the lysosome for degradation. These findings implicate a novel role for c-Abl and Hsc70 as an unexpected regulator of Hsc70-mediated transport of trophic receptor cargo between the early and late endosomal compartments.

Iron homeostasis is an essential physiological process for all cells and tissues, and the hepatocyte plays a central role in the liver's capacity to regulate iron levels for the entire body. To this end, it employs two receptors, the transferrin receptors 1 and 2 (TfR1 and TfR2), that promote internalization of iron-bound transferrin (Tf)[3] as well as stimulation of iron transporters in other cells and tissues (1–5). TfR1 is expressed in almost all cells and tissues and is dependent on canonical endocytic machinery for internalization, trafficking, sorting, and recycling to the plasma membrane (6, 7). In contrast, TfR2 may enter the hepatocyte by several endocytic mechanisms and is directed to the lysosome for degradation (8, 9).

Although most receptor tyrosine kinases (RTKs) upon ligand addition undergo a highly regulated endocytic process of internalization, which is controlled by phosphorylation and other post-translational modifications, TfR1 endocytosis has been thought to persist continuously in an ongoing or "constitutive" process. However, recent studies by us and others (10, 11) have suggested that the binding of the Tf ligand leads to the activation of Src kinase, which in turn promotes phosphorylation of specific components of the endocytic machinery such as dynamin 2 (Dyn2) and its actin-associated binding partner cortactin (12–16). The Src-mediated phosphorylation event of these specific endocytic components appears to be essential for efficient assembly and scission of clathrin-coated pits that are utilized to internalize this receptor-ligand complex.

To test whether other levels of regulation might exist at additional stages of TfR1 trafficking, we initiated a simple screen to define the effects of inhibiting other non-receptor tyrosine kinases (NRTKs) on Tf internalization. Subsequently, we observed that treating different cultured hepatocyte cell lines with imatinib (17, 18), a potent inhibitor of the c-Abl family of NRTKs, resulted in a near complete ablation of ligand uptake. More specific inhibition of c-Abl function through expression of inhibitory mutants and/or the use of c-Abl knock-out (KO) mouse embryonic fibroblasts (MEFs) both appear consistent with the concept that functional c-Abl is indispensable for Tf-TfR1 internalization. Surprisingly, the effects of c-Abl loss on TfR1 internalization appeared not to be an endocytic block, but rather a near total removal of TfR1 from the cell surface. Cell and biochemical studies designed to track the fate of the internalized receptor-ligand complex indicated that in the absence

* This work was supported by National Institutes of Health Grants DK44650 (to M. A. M.), T32DK007352 (to M. B. S.), and DK84567 (to the Optical Microscopy Core of the Mayo Center for Cell Signaling in Gastroenterology). The authors declare that they have no conflicts of interest with the contents of this article. The content is solely the responsibility of the authors and does not necessarily represent the official views of the National Institutes of Health.

[S] This article contains supplemental Figs. S1–S5.

[1] Present address: Technical if Munich, Chair of Biological Imaging, Ismaninger Str. 22, 81675 Munich, Germany.

[2] To whom correspondence should be addressed: Dept. of Biochemistry and Molecular Biology, Mayo Clinic, 200 First St. SW, Guggenheim 1642D, Rochester, MN 55905. Tel.: 507-284-0683; Fax: 507-284-2053; E-mail: mmcniven@mayo.edu.

[3] The abbreviations used are: Tf, transferrin; TfR, transferrin receptor; NRTK, non-receptor tyrosine kinase; EGFR, epidermal growth factor receptor; RTK, receptor tyrosine kinase; MEF, mouse embryonic fibroblast; IF, immunofluorescence; PES, 2-phenylethyne sulfonamide; LDLR, LDL receptor; Ub, ubiquitin; MVB, multivesicular body.

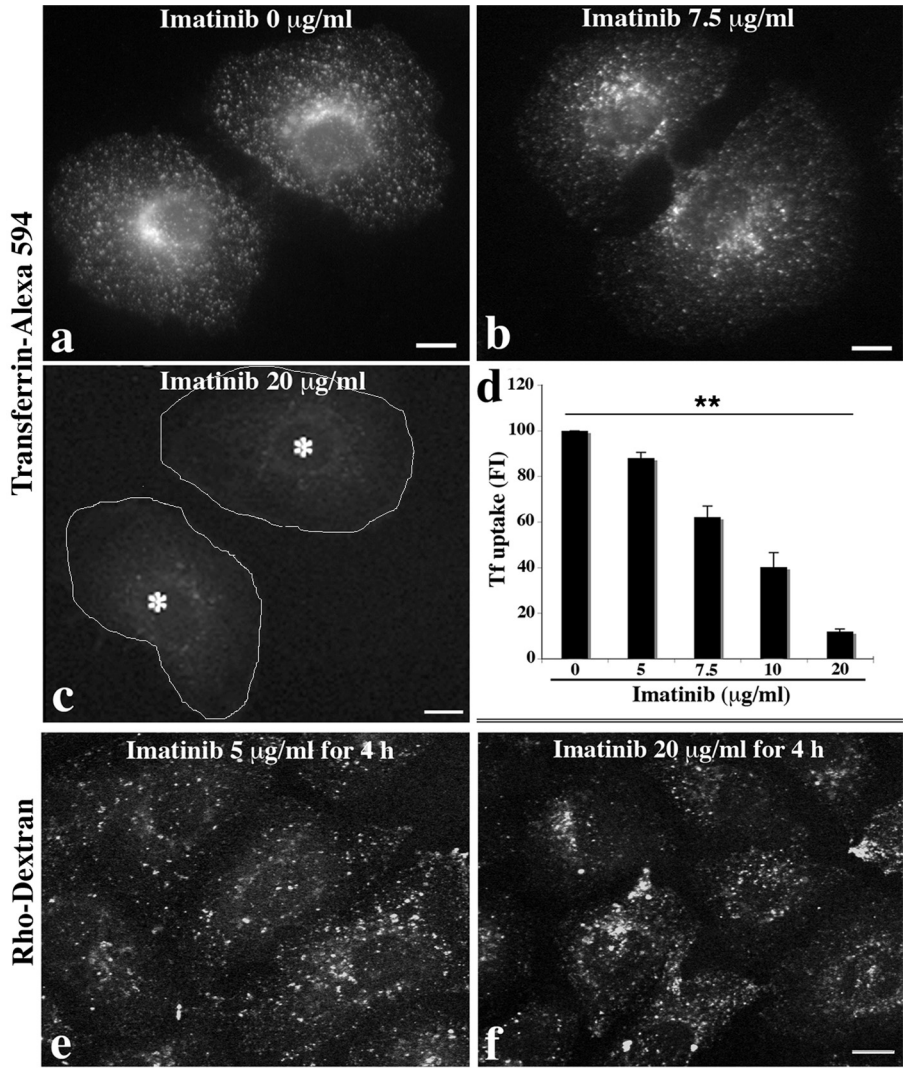

FIGURE 1. **Inhibition of c-Abl kinase by imatinib interferes with the endocytic uptake of transferrin but not the fluid phase marker dextran.** *a–c,* effects of imatinib on Tf internalization in clone 9 cells pre-treated with various concentrations of the drug for 2 h, then incubated with Alexa-594-labeled Tf for 20 min, and analyzed by fluorescence microscopy. Note that imatinib interferes with Tf internalization in a dose-dependent manner. Cells in *c* are outlined and marked with an *asterisk* due to low fluorescence intensity. *d,* quantitation of Tf uptake from three independent experiments as described in *a–c*. Results are presented as mean ± S.E. with >50 cells measured per condition. **, $p < 0.01$. *e–f,* clone 9 cells were pre-treated for 2 h with 5 μg/ml (*e*) or 20 μg/ml imatinib (*f*) and incubated for an additional 2 h with 150 mM rhodamine-conjugated dextran and analyzed by fluorescence microscopy. Note that in contrast to Tf uptake, imatinib treatment does not affect fluid phase internalization. *Scale bars,* 10 μm.

of c-Abl kinase activity, the TfR1 is not recycled back to the cell surface as usual, but instead is re-directed to the degradative pathway, resulting in the observed reduction in the receptor levels. Parallel studies with the LDL receptor show a similar lysosome-based degradation upon inhibition of c-Abl. Interestingly, c-Abl inhibition promoted a strong interaction of Tf-TfR1 with the cytoplasmic chaperone Hsc70, suggesting that this interaction may be responsible for redirecting this receptor from the perinuclear recycling endosome to the lysosome. Pharmacological inhibition of Hsc70 activity in c-Abl attenuated cells prevents this interaction, resulting in a diffuse distribution of the chaperone, although the receptor accumulates in the early endosome, suggesting that Hsc70 is required for the trafficking of the TfR1 from the early to late endosome upon c-Abl inhibition. These data support the concept that c-Abl plays an important role in directing the endocytic fate of the TfR1 and other receptors.

Results

c-Abl Kinase Activity Is Required for Efficient Internalization of Transferrin—We previously reported that the initial steps of TfR1 internalization are regulated by the action of the NRTK Src (11). Based on these findings, we examined a subset of inhibitors of other NRTKs on Tf internalization to identify additional regulators of receptor-mediated endocytosis. Surprisingly, out of the various compounds tested, imatinib, a widely used and relatively specific inhibitor of c-Abl kinase (17–21), appeared most effective in reducing Tf endocytosis when tested in clone 9 rat hepatocytes. As shown in Fig. 1, *a–c*, imatinib treatment prevented Tf internalization in these cells in a dose-dependent manner as measured by quantitation of total fluorescence intensity assayed 20 min post-application of the ligand (Fig. 1*d*). The inhibitory effect appeared to be specific for receptor-mediated

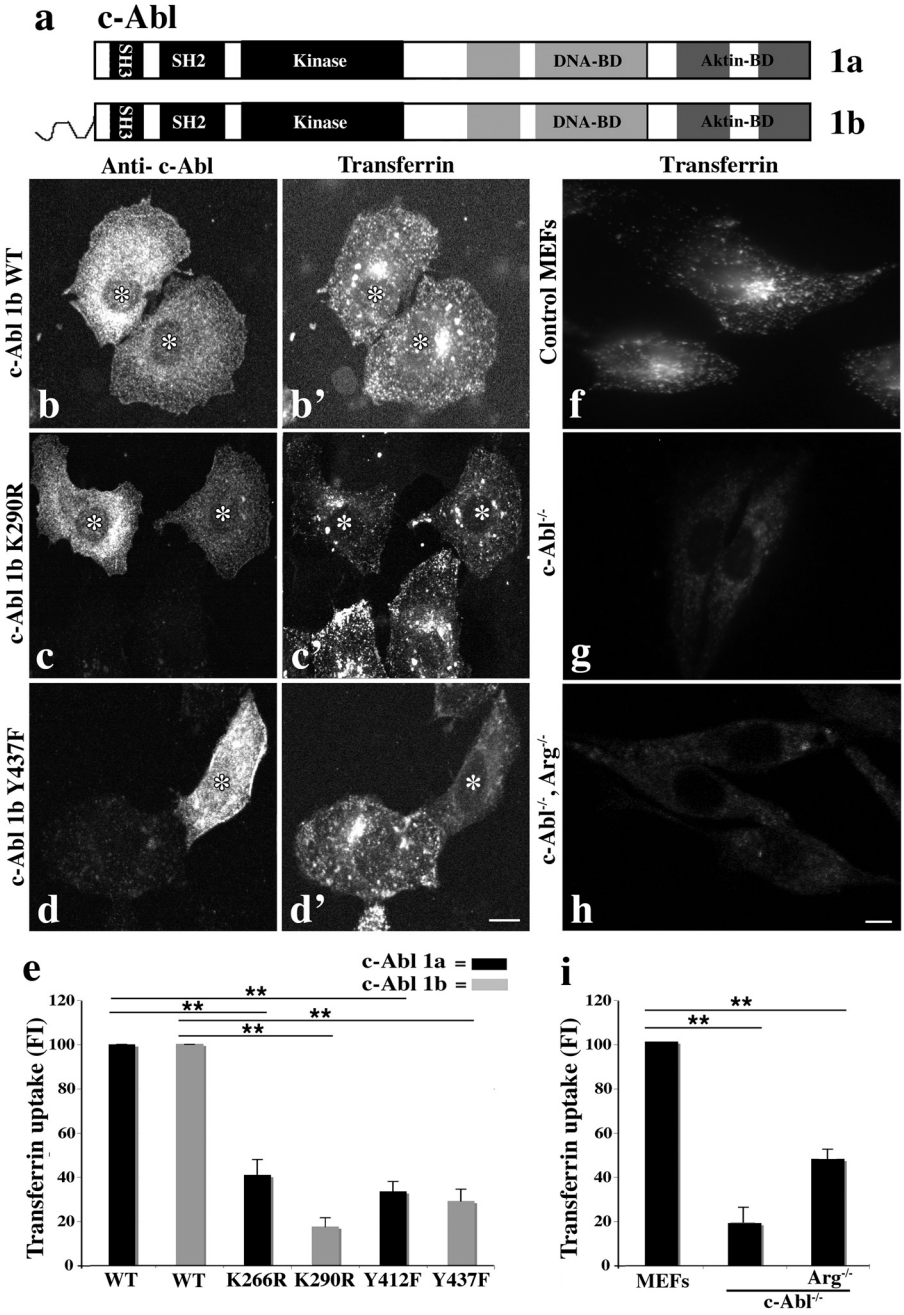

FIGURE 2. **Endocytic internalization of Tf is reduced significantly in cells lacking functional c-Abl kinase.** *a,* schematic illustrating the domain structures of c-Abl-1a and c-Abl-1b. Both proteins are comprised of Src homology domain 3 (*SH3*) and Src homology domain 2 (*SH2*) followed by the tyrosine kinase domain. The two splice variants differ in their N terminus, which is myristoylated in the 1b form, but this modification is absent in the shorter 1a variant. *b–d″* endocytic uptake of Alexa-594-labeled Tf in clone 9 cells expressing either wild-type c-Abl-1b (*b* and *b′*), a kinase-dead mutant K290R (*c* and *c′*), or the inactive mutant Y437F (*d* and *d′*). Transfected cells (*asterisks*) were visualized by staining with antibodies against c-Abl and were analyzed by fluorescence microscopy (*b–d′*). Note that cells expressing non-functional forms of c-Abl internalized significantly less Tf than adjacent untransfected cells or cells expressing WT c-Abl. *e,* quantitation of Tf uptake as described in *b–d′* by measurement of total fluorescence. Data represent the mean ± S.E. from three independent experiments with >50 cells measured for each condition. **, $p < 0.01$. *Scale bars,* 10 μm. *f–h,* control MEFs (*f*), c-Abl$^{-/-}$ single KO (*g*), and c-Abl$^{-/-}$, Arg$^{-/-}$ double KO MEFs (*h*) were incubated with Alexa-594-labeled Tf for 20 min, acid-stripped, and subsequently analyzed by fluorescence microscopy. *Scale bar,* 10 μm. *i,* quantitation of Tf uptake based on fluorescence intensity measurements in these cells. Note that Tf internalization is markedly reduced in both c-Abl$^{-/-}$ single and c-Abl$^{-/-}$, Arg$^{-/-}$ double KO MEFs, compared with control cells. Data represent the mean ± S.E. from three independent experiments with > 50 cells measured for each condition. **, $p < 0.01$.

endocytosis, as fluid phase uptake, assessed by rhodamine-dextran (M_r 3,000) internalization for 2 h, was unaffected by imatinib treatment (Fig. 1, *e* and *f*).

As pharmacological inhibitors may result in a number of non-specific effects, two alternative approaches were taken to confirm the inhibitory effects of imatinib on TfR1 internalization. First, clone 9 cells were transfected to overexpress either WT, the kinase-dead K266R/290R mutant, or the inactive 419/437F form (22, 23) of both splice variants of c-Abl (c-Abl-1a and -1b, Fig. 2*a*) (24, 25), and Tf internalization was allowed for 20 min before the cells were acid-stripped and further analyzed. Consistent with our findings using imatinib, expression of a

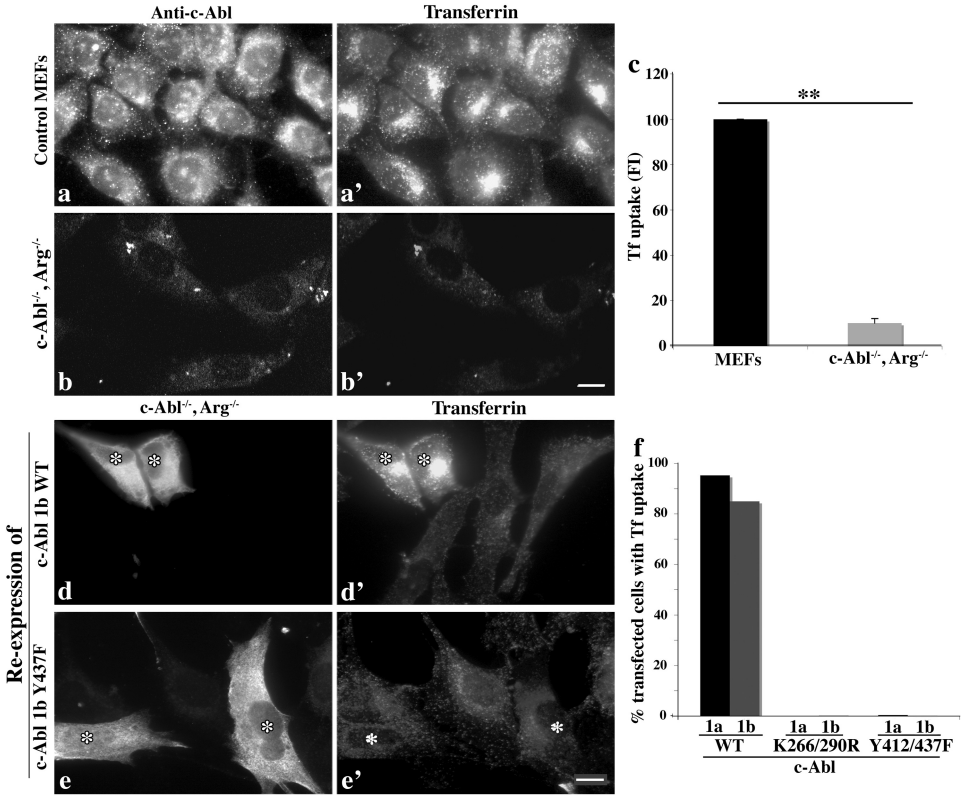

FIGURE 3. **Expression of functional c-Abl rescues Tf internalization in Abl$^{-/-}$, Arg$^{-/-}$ double KO MEFs.** Control MEFs (*a* and *a′*) and c-Abl$^{-/-}$, Arg$^{-/-}$ KO MEFs (*b* and *b′*) were challenged to internalize Alexa-594-labeled Tf (*a′* and *b′*) for 20 min and subsequently analyzed by fluorescence microscopy. *c,* quantitation of three independent experiments as described in *a* show that only negligible amounts of Tf were internalized by the double KO cells compared with the control cells. Data are presented as mean ± S.E. with over 100 cells measured per condition. **, $p < 0.01$. *d–e′*, re-expression of c-Abl restores Tf uptake in c-Abl$^{-/-}$, Arg$^{-/-}$ MEFs. Cells were transfected with WT c-Abl-1b (*d*) or the inactive mutant Y412F (*e*), and the expression of the c-Abl proteins (cells are marked with *asterisks*) was detected by immunofluorescence using an anti-c-Abl antibody. Importantly, c-Abl WT, but not the inactive mutant, was able to rescue the defective Tf internalization in the KO MEFs. *f,* quantitation of the three independent experiments as described in *d–e′*. Included in the analysis here are also the kinase-dead mutants of the two c-Abl isoforms (Lys-266 and Lys-290), respectively. Data are presented as mean ± S.E. and >100 cells were counted per condition. **, $p < 0.01$ *Scale bars,* 10 μm.

non-functional c-Abl-1b (K290R or Y437F) induced a dramatic defect in Tf uptake compared with c-Abl WT-expressing control cells (~60% reduction, Fig. 2, *b–e*). No significant difference was observed between the two c-Abl splice variants, suggesting that myristoylation of the kinase, and thus membrane anchoring, is not an important factor in the c-Abl-mediated regulation of Tf uptake (Fig. 2*e*). In a second approach, Tf internalization was assessed in both c-Abl knock-out MEFs (c-Abl$^{-/-}$) and c-Abl/Arg double knock-out (c-Abl$^{-/-}$, Arg$^{-/-}$) MEFs compared with control MEFs. As shown in Fig. 2, *f–h*, Tf endocytosis was greatly diminished (~50–80%, Fig. 2*i*) in cells depleted of c-Abl or c-Abl/Arg compared with control cells.

Based on these data, we predicted that re-expression of c-Abl WT, but not the inactive mutants, would restore Tf internalization in c-Abl$^{-/-}$ MEFs. To this end, c-Abl WT or the non-functional mutants (Y419F/Y437F or K266R/K290R) were re-expressed in the c-Abl$^{-/-}$ MEFs, and Tf uptake was analyzed by immunofluorescence microscopy as described above, and the expression of the various c-Abl constructs was verified using a specific antibody to the kinase (Fig. 3, *a–e*). As predicted, the internalization defect in the KO cells (Fig. 3, *a′*, *b′*, and *c*) was rescued by re-expression of c-Abl-1b WT, but not the inactive (Y437F) or the kinase-dead (K290R) mutant (Fig. 3, *d* and *e′*), suggesting that active c-Abl kinase is required to promote Tf uptake. Again, both c-Abl splice variants rescued Tf uptake with equal efficiency (Fig. 3*f*). Taken together, using three different approaches, these data suggest that functional kinase-active c-Abl is essential for efficient Tf internalization.

Inhibiting c-Abl Results in a Reduction of Surface TfR1—Although the findings described above suggest a requirement for c-Abl activity in the endocytic internalization of the TfR1, an alternative explanation for the marked attenuation in Tf uptake could be a reduction in numbers of cell surface receptors. To test this, we first examined the surface levels of the TfR1 in the presence or absence of imatinib, both biochemically and by immunofluorescence microscopy. Surprisingly, inhibition of c-Abl by imatinib caused a dramatic reduction (~70%) in surface TfR1, both by IF with an antibody that recognizes the TfR1 extracellular domain (Fig. 4, *a–c*) and biochemical analysis using a surface biotinylation assay (Fig. 4, *d* and *e*). To extend this finding, total cellular TfR1 levels were compared in control *versus* c-Abl$^{-/-}$ KO MEFs and were found to be greatly reduced, even below the detection limits of the Western blotting analysis (Fig. 5*a*). Most importantly, re-expression of c-Abl WT (splice variants 1a and 1b, Fig. 5*b*) in the c-Abl KO MEFs restored TfR1 levels close to that of the control MEFs (Fig. 5*c*) and subsequently rescued uptake of the Tf ligand (Fig. 5, *d–g′*). These observations are consistent with the concept that c-Abl

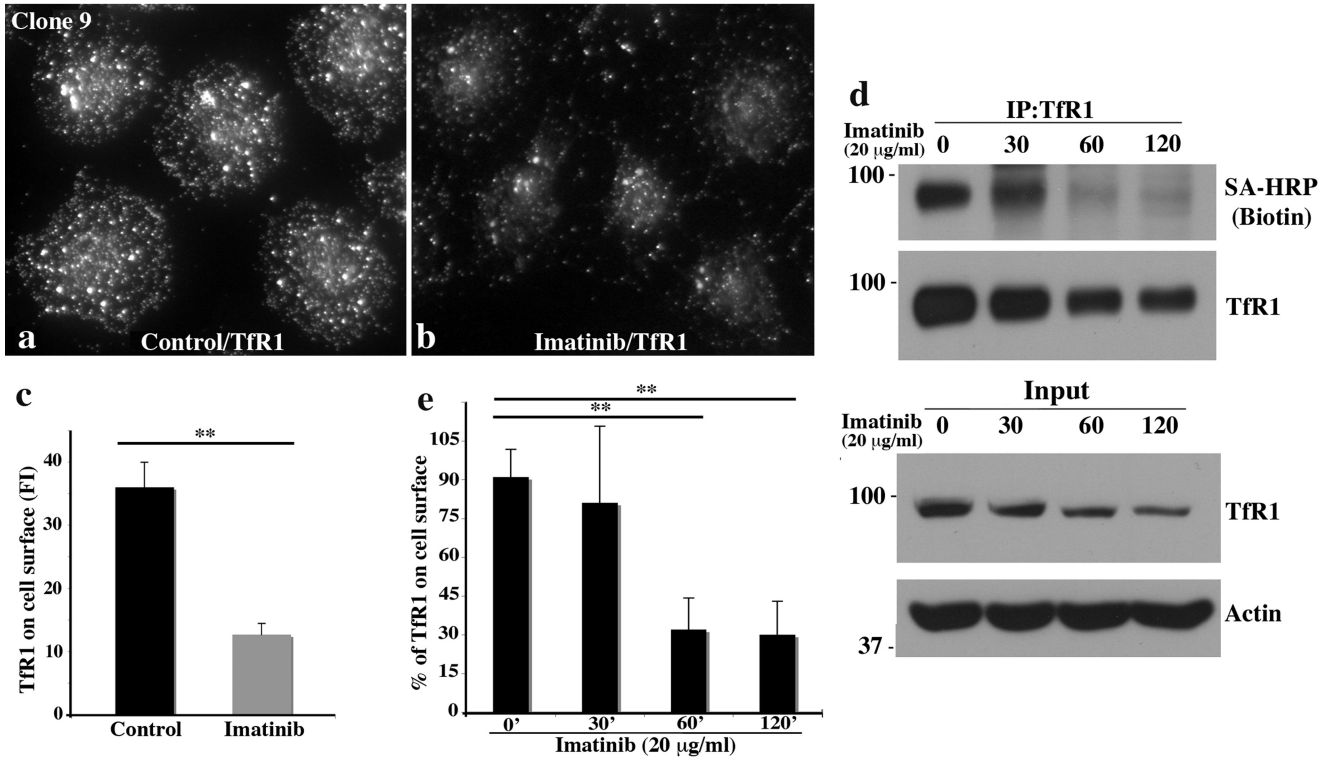

FIGURE 4. **Imatinib treatment causes a reduction in surface TfR1 levels.** *a* and *b*, inhibition of c-Abl kinase activity by imatinib reduces TfR1 surface levels. Control (*a*) or imatinib-treated clone 9 cells (*b*) were analyzed by indirect immunofluorescence without permeabilization using an antibody against the extracellular domain of the TfR1. *Scale bars,* 10 μm. *c,* quantitation of three independent experiments as described in *a* and *b*. Data are presented as mean ± S.E. from >50 cells per condition. **, $p < 0.01$. Notably, there is a significant reduction in surface TfR1 levels following imatinib treatment compared with control cells. *d,* biochemical assessment of surface TfR1 by a biotinylation assay. The levels of biotinylated surface TfR1 *versus* total cellular TfR1 in control and drug treated cells were analyzed by Western blot. A representative blot of three different experiments is provided and shows a dramatic loss of surface TfR1 60 min post-imatinib treatment. Also, note a substantial reduction in total cellular TfR1 levels that occurs in response to the drug. *IP*, immunoprecipitation. *e,* quantitation of three independent experiments as described in *d*. Data are presented as mean ± S.E. and reveal a dramatic reduction in surface TfR1 levels following imatinib treatment. For all time points, surface TfR1 was normalized to total TfR1. **, $p < 0.01$.

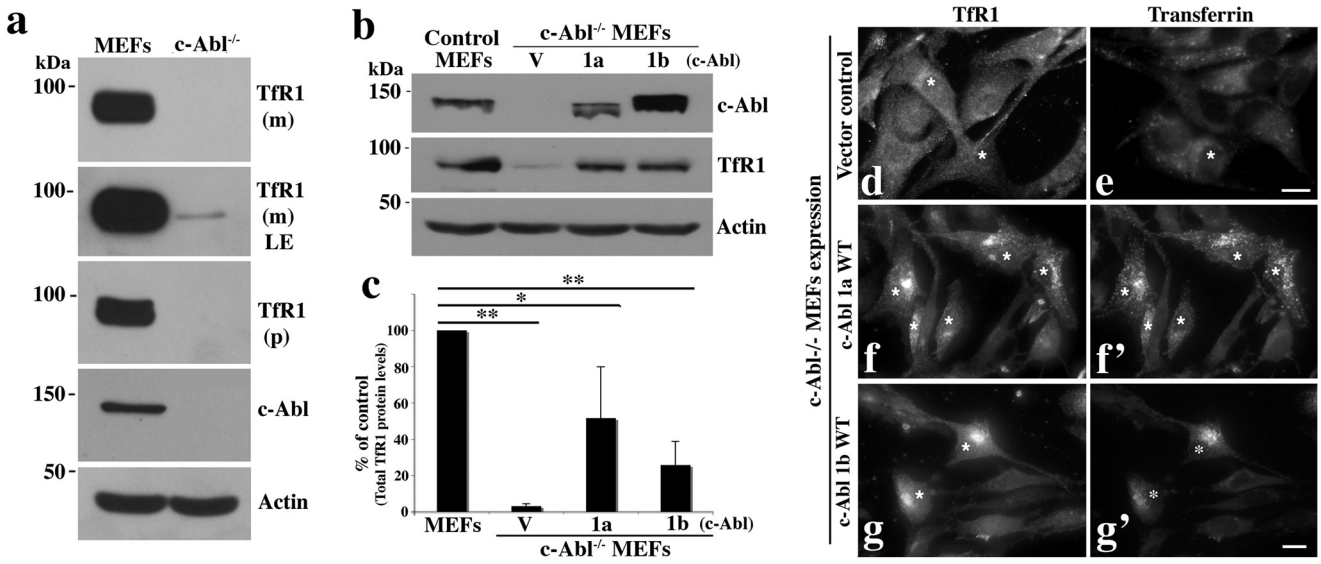

FIGURE 5. **Re-expression of c-Abl kinase restores TfR1 levels and Tf internalization in c-Abl$^{-/-}$ MEFs.** *a,* Western blotting analysis of TfR1 levels in control MEFs and c-Abl$^{-/-}$ KO MEFs. Endogenous levels of c-Abl kinase and TfR1 were assessed by specific antibodies to each protein. *m,* monoclonal antibody; *p,* polyclonal antibody; *LE,* long exposure. *b,* although little, if any, TfR1 is observed in the c-Abl-negative cells, re-expression of the WT form of the 1a or the 1b splice variant of c-Abl kinase restored TfR1 expression. *c,* quantitation of three independent experiments as described in *b*. Data are presented as mean ± S.E.; *, $p < 0.05$, **, $p < 0.01$. *d* and *e,* c-Abl$^{-/-}$ KO MEFs expressing control vector (GFP) were allowed to internalize Alexa-594-labeled Tf (*e*) for 20 min, acid-stripped, and stained with anti-TfR1 antibody. *f–g′,* c-Abl$^{-/-}$ KO MEFs re-expressing wild-type c-Abl-1a (*f*) or cAbl-1b (*g*) were allowed to internalize Alexa-594-labeled Tf (*f′–g′*) for 20 min, acid-stripped, and stained with anti-c-Abl (not shown, cells marked by an *asterisk*) and anti-TfR1 antibodies (*f* and *g*) for further analysis by fluorescence microscopy. Of note, re-expression of WT c-Abl can to restore both TfR1 protein levels (*f* and *g*) and Tf uptake (*f′* and *g′*) in c-Abl$^{-/-}$ KO MEFs. *Scale bar,* 10 μm.

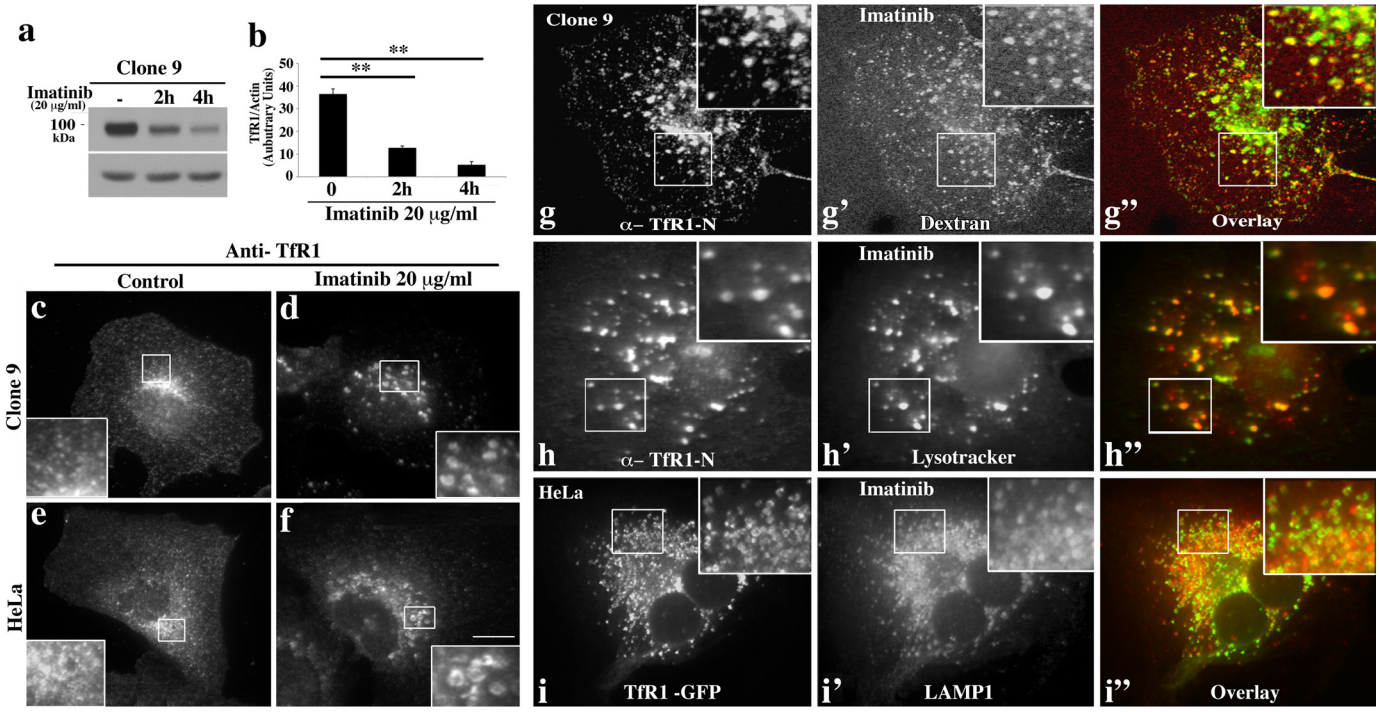

FIGURE 6. **TfR1 is targeted to the lysosome in response to c-Abl inhibition.** *a,* treatment of clone 9 cells with imatinib causes a loss of total TfR. Clone 9 cells treated with 20 μg/ml imatinib over different time periods (0, 2, and 4 h) were subjected to Western blotting analysis using an antibody to TfR1. A dramatic and stepwise reduction of TfR1 levels was observed resulting in an almost complete loss of the receptor by 4 h post-treatment as confirmed by densitometric quantitation of three different experiments. *b*, **, $p < 0.01$. *c–f,* immunofluorescence images of clone 9 or HeLa cells under control conditions (*c* and *e*) or treated with 20 μg/ml imatinib for 2 h (*d* and *f*). Control cells show a punctate endosomal plasma membrane-associated as well as the typical peri-nuclear pool of the TfR1. In contrast, imatinib-treated cells sequestered the TfR1 into large circular structures often with a dark unstained center (*d* and *f*; *insets*). *g–g″*, TfR1 resides in dextran-positive endosomes in imatinib-treated cells as visualized after pulse-chase labeling of endosomes and costaining of endogenous TfR1. *h* and *h′*, clone 9 cells were pre-treated with LysoTracker Deep Red (1 μM) in medium for 1 h. TfR1 resides in LysoTracker-positive compartment in imatinib treated cells as visualized by staining of endogenous TfR1. *i–i″*, imatinib-treated HeLa cells expressing GFP tagged TfR1 (*i*) were analyzed by indirect immunofluorescence using an antibody against the lysosomal marker LAMP1 (*i′*). An obvious co-labeling of TfR1 with late endosomes/lysosomes is observed (*i–i″*), indicative of receptor "mis-sorting" to the lysosome upon inhibition of c-Abl kinase. *Scale bars,* 10 μm.

does not regulate Tf endocytosis directly, but possibly by altering the surface availability of this important trophic receptor.

TfR1 Is Targeted to the Lysosome for Degradation upon Imatinib Treatment—To confirm that imatinib treatment also reduces total cellular TfR1 levels and to gain an appreciation for how quickly any potential loss might occur, clone 9 cells were treated with 20 μg/ml imatinib over different time points (0, 2, and 4 h) and subjected to Western blotting analysis (Fig. 6*a*). Interestingly, by just 2 h post drug treatment, receptor levels were reduced by 50% and almost completely ablated by 4 h (Fig. 6*b*).

This observed reduction in TfR1 levels upon imatinib treatment suggested that an alteration in endocytic trafficking occurs upon inhibition of c-Abl that minimizes the recycling of the internalized receptor back to the surface, while potentially promoting its transport to the lysosome for subsequent degradation. To test for c-Abl-dependent changes in the intracellular localization of the endocytosed receptor that might support this premise, clone 9 (Fig. 6, *c* and *d*) or HeLa cells (Fig. 6, *e* and *f*) were treated with 20 μg/ml imatinib for 2 h prior to fixation and stained for TfR1. As hypothesized, a marked redistribution of internalized receptor was observed from the canonical perinuclear recycling compartment seen in control cells (Fig. 6, *c* and *e*) to large discrete vesicles reminiscent of a late endosomal/lysosomal compartment in the cells exposed to imatinib (Fig. 6, *d* and *f*). To determine the nature of this compartment, clone 9 cells were pulse-labeled for 2 h with 150 mM rhodamine-dextran (M_r 3,000) to visualize late endosomes/lysosomes. Interestingly, 2 h post imatinib treatment, TfR1 showed a striking colocalization with both dextran-positive compartments (Fig. 6, *g–g″*) or the Lysotracker dye (Fig. 6, *h–h″*). Moreover, the expressed GFP-tagged TfR1 clearly associated with GFP-LAMP1-positive structures (Fig. 6, *i–i″*), suggesting that indeed TfR1 is re-directed from its "normal" recycling route to the degradative pathway in the presence of imatinib. To test whether c-Abl inhibition might have similar effects on other trophic receptors, parallel experiments were performed on cells to observe alterations in the trafficking of the LDL receptor. It has been well documented that upon ligand binding, this receptor is trafficked through the endocytic pathway to an acidic compartment that mediates the dissociation, sorting, and recycling of a percentage of this receptor back to the cell surface, although its lipid cargo progresses to the lysosome for degradation (26). Because of this partial receptor recycling, we viewed the LDLR as a suitable comparison with the TfR1. As displayed in supplemental Fig. S1, clone 9 cells treated with 20 μg/ml imatinib over different time periods (0, 2, and 4 h) were subjected to Western blotting analysis using an antibody to LDLR. A stepwise reduction of LDLR levels was observed post-treatment in a time frame similar to that of the TfR1. In support of these findings, IF-based analysis demonstrated that cells treated with vehicle or 20 μg/ml imatinib for 2 h exhibit a

plasma membrane-associated punctate endosomal pool as well as the typical peri-nuclear pool of the LDLR. In contrast, imatinib-treated cells sequester the LDLR into large circular structures that stain positive for the lysosomal marker LAMP1. Thus, the recycling of both the TfR1 and LDLR appear to be "missorted" to the lysosome upon inhibition of c-Abl kinase.

To provide a functional test that imatinib-induced reduction in TfR1 levels is due to lysosomal degradation, lysosome function was inhibited via the H^+-ATPase inhibitor bafilomycin. Accordingly, clone 9 cells were pre-treated with bafilomycin (1 μM, 2 h) followed by treatment with imatinib (20 μg/ml for 0, 2, and 4 h) and subjected to Western blotting analysis for TfR1 (Fig. 7). As predicted,

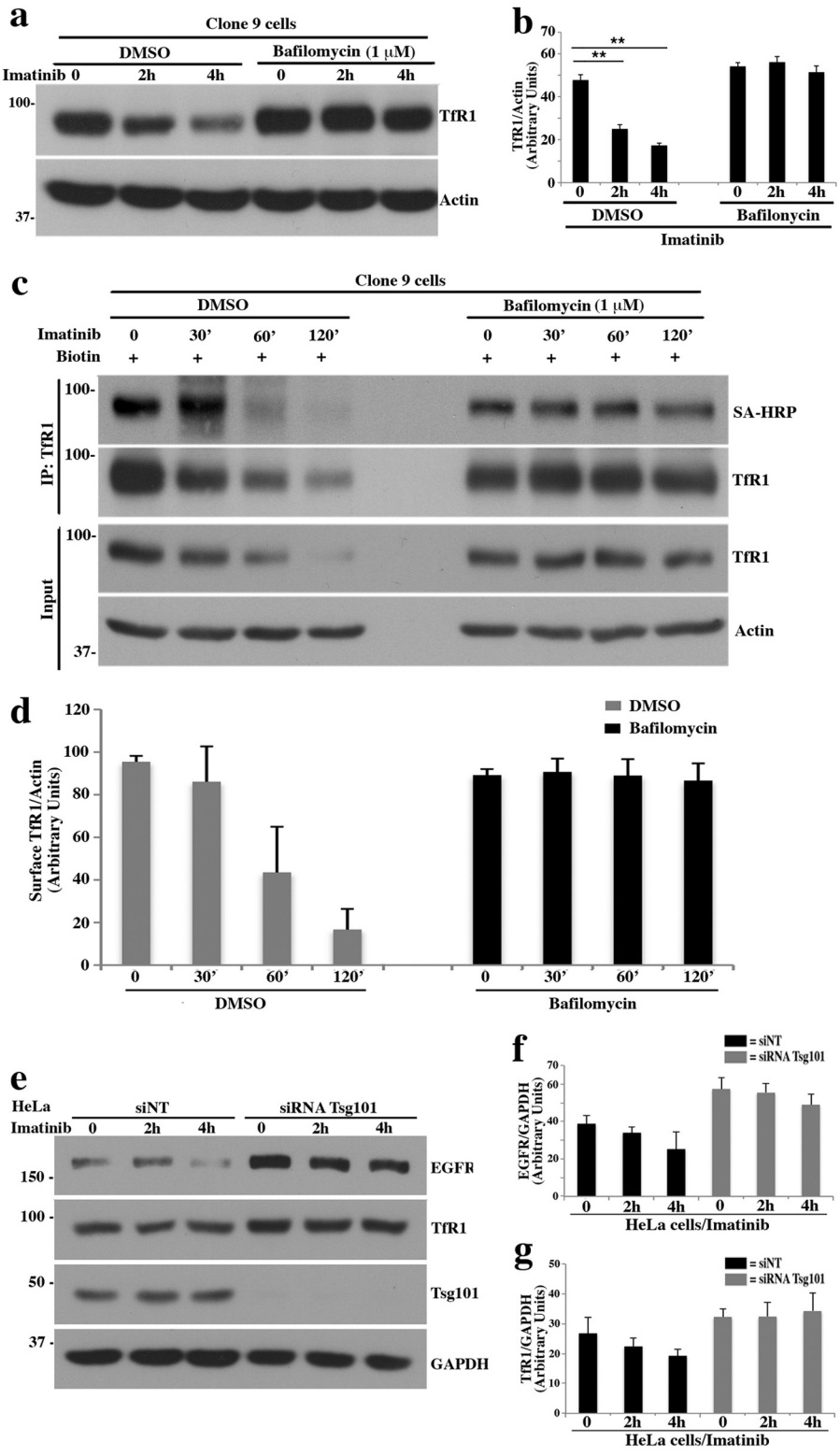

a substantial stepwise reduction of TfR1 levels by imatinib was observed in control cells pretreated with DMSO (Figs. 6, *a* and *b*, and 7, *a* and *b*), but this loss was completely prevented in cells that were pre-treated with bafilomycin (Fig. 7, *a* and *b*). In addition, pre-treatment with bafilomycin prevented the loss of surface TfR1 levels by exposure to imatinib (Fig. 7, *c* and *d*). Additional experiments using the lysosomal protease inhibitor leupeptin also showed a marked, but not complete, protection of the TfR1 in imatinib-treated cells (supplemental Fig. S2). Consistent with these findings, LDLR levels were also largely maintained by bafilomycin both in cells treated with imatinib and also in c-Abl$^{-/-}$ MEFs (supplemental Fig. S3).

These findings led us to test how TfR1 might be targeted to the lysosome, a pathway that is normally used by the TfR2 via Ub-mediated mechanisms (27). To test whether TfR1 is ubiquitylated following c-Abl inhibition, Hep3b or HeLa cells were transfected with HA-Ub for 16 h, then pre-treated with bafilomycin (2 h), and treated with imatinib (20 μg/ml, 2 h). The premise of this approach was to activate any Ub-based targeting of the TfR1 via inhibition of c-Abl but to retain high levels of this putatively tagged receptor by inhibiting the degradative function of the lysosome with bafilomycin. Treated cells were then homogenized and subjected to immunoprecipitation for the TfR1 or the EGFR as a positive control, followed by Western blotting analysis for HA. Although the EGFR displayed significant ubiquitylation even in the absence of added ligand, no detectable modification was observed for the TfR1 (data not shown).

To further test a role for a ubiquitin-based transport of the TfR1 to the lysosome, we attempted to disrupt the ESCRT-based trafficking of cargo to the MVB via an siRNA-based knockdown of Tsg101, a component of the ESCRT1 complex that recognizes ubiquitylated cargo (28). HeLa cells treated with an siRNA to Tsg101 for 3 days were then challenged to internalize and degrade either the TfR1 or EGFR following imatinib treatment for 0, 2, and 4 h, as depicted in Fig. 7, *e–g*. Although the stepwise loss of these receptors is observed in siNT cells, those with reduced levels of Tsg101 are impaired in receptor loss, suggesting a functional role for the ESCRT complex in this process.

Activation of an Hsc70 Chaperone-based Pathway to the Lysosome—As an alternative to the canonical ubiquitylation pathway, we tested for a functional role of the cytoplasmic chaperone Hsc70, which is known to facilitate the transport of many proteins to the lysosome, among them the EGFR (29), by a mechanism referred to as chaperone-mediated autophagy (30, 31). Coimmunoprecipitation assays were performed in clone 9 cells in the presence or absence of imatinib (20 μg/ml, 2 h; Fig. 8, *a* and *b*). Surprisingly, TfR1 from imatinib-treated cells precipitated substantially more Hsc70 than did control cells, whereas a reciprocal immunoprecipitation of Hsc70 exhibited an even greater association with TfR1 (5-fold) in the imatinib-treated cells (Fig. 8, *a′* and *b′*) compared with the vehicle-treated controls. To test whether this increased interaction might be resolved by microscopy in fixed cells, clone 9 cells expressing GFP-Hsc70 were treated with 20 μg/ml imatinib for 2 h and immunostained for the TfR1 (Fig. 8, *c–d″*) or in GFP-LAMP1 cells expressing clone 9 cells immunostained for Hsc70 (Fig. 8, *e–f″*). Although the Hsc70 chaperone appeared diffuse in control cells (Fig. 8*c*), imatinib treatment induced the formation of vesicle-like puncta (Fig. 8*d*) that exhibited substantial overlap with internalized TfR1 (Fig. 8*d″*).

As we have shown that inhibition of c-Abl induces targeting of the internalized TfR1 to lysosomes, imatinib-treated cells expressing GFP-tagged LAMP1 revealed a clear colocalization between Hsc70 puncta and the LAMP1-positive lysosomes (Fig. 8, *f* and *f″*) that was not observed in control cells (Fig. 8, *e′* and *e″*). To provide a functional test for involvement of Hsc70 in imatinib-induced TfR1 degradation, we utilized a small molecule ATP-derivative inhibitor of Hsc/Hsp70 chaperones (VER155008) that is well described to have antitumor properties (32). Importantly, we found that this inhibitor minimizes the imatinib-dependent TfR1 degradation by lysosomes. Clone 9 cells were pre-treated with DMSO or the Hsc70 inhibitor VER155008 (100 μM) for 16 h, treated with 20 μg/ml imatinib over different time periods (0, 2, and 4 h), and subjected to Western blotting analysis for TfR1 levels (Fig. 9, *a* and *b*). Inhibiting c-Abl induced the stepwise loss of the receptor in the DMSO-treated control cells, whereas inhibiting Hsc70 function with VER155008 substantially prevented this loss.

To test whether the Hsc70 inhibitor VER155008 reduces the TfR1-Hsc70 interaction as observed in Fig. 8*b*, cells were treated as described above but subjected to co-IP of Hsc70 and were analyzed by Western blotting (Fig. 9, *c* and *d*). Total protein shown in the input lanes exhibits a protection of the TfR1 by the Hsc70 inhibition as in Fig. 9, *a* and *b*, whereas receptor and chaperone reveal a significantly reduced association when Hsc70 function is inhibited, despite the fact that the levels of this protein are increased. From these findings it became important to define whether the cellular distribution of these proteins was altered by VER155008-mediated chaperone inhibition. Clone 9 cells were pretreated overnight with carrier

FIGURE 7. **The lysosome inhibitor, bafilomycin, reduces TfR1 degradation in imatinib-treated cells.** *a,* bafilomycin prevents lysosomal degradation of the TfR1. Clone 9 cells were pre-treated with the lysosome inhibitor bafilomycin (1 μM) for 2 h, treated with 20 μg/ml imatinib over different time periods (0, 2, and 4 h), and then subjected to Western blotting analysis using an antibody to TfR1. As observed previously, imatinib induced a dramatic and stepwise reduction of TfR1 levels, but this reduction is attenuated almost completely in the presence of bafilomycin, as quantified by densitometry from three different experiments. *b,* **, $p < 0.01$. *c,* TfR1 surface levels are maintained in bafilomycin-treated cells as assessed by a surface biotinylation assay. As described in Fig. 4, the levels of biotinylated surface TfR1 *versus* total cellular TfR1 in control (imatinib) and bafilomycin treated cells were analyzed by Western blot. A representative blot of three different experiments is provided and shows a dramatic loss of surface TfR1 60 min post-imatinib treatment. Also, there is a substantial reduction in total cellular TfR1 levels that occurs in response to imatinib. In contrast, the lysosome inhibitor, bafilomycin, prevents TfR1 loss of both total cellular and surface receptor. Quantitation of three independent experiments as described in *d*. Data are presented as mean ± S.E. and reveal a dramatic reduction in surface TfR1 levels following imatinib treatment. For all time points, surface TfR1 was normalized to total TfR1. **, $p < 0.01$. *e–g,* c-Abl inhibitor imatinib-induced loss of the TfR1 is dependent upon the ESCRT1 component Tsg101. *e,* Western blotting analysis of HeLa cells pre-treated with Tsg101 siRNA for 3 days and then treated with 20 μg/ml imatinib over different time periods (0, 2, and 4 h) preceding cell lysis, SDS-PAGE, and blotting with antibodies to TfR1, EGFR, and Tsg101. As observed previously, imatinib induced a reduction in receptor levels, an effect that was nearly ablated by the pre-treated with Tsg101 siRNA. EGFR is provided as a positive control comparison. *f* and *g,* corresponding *graphs* represent densitometric quantification of three different experiments.

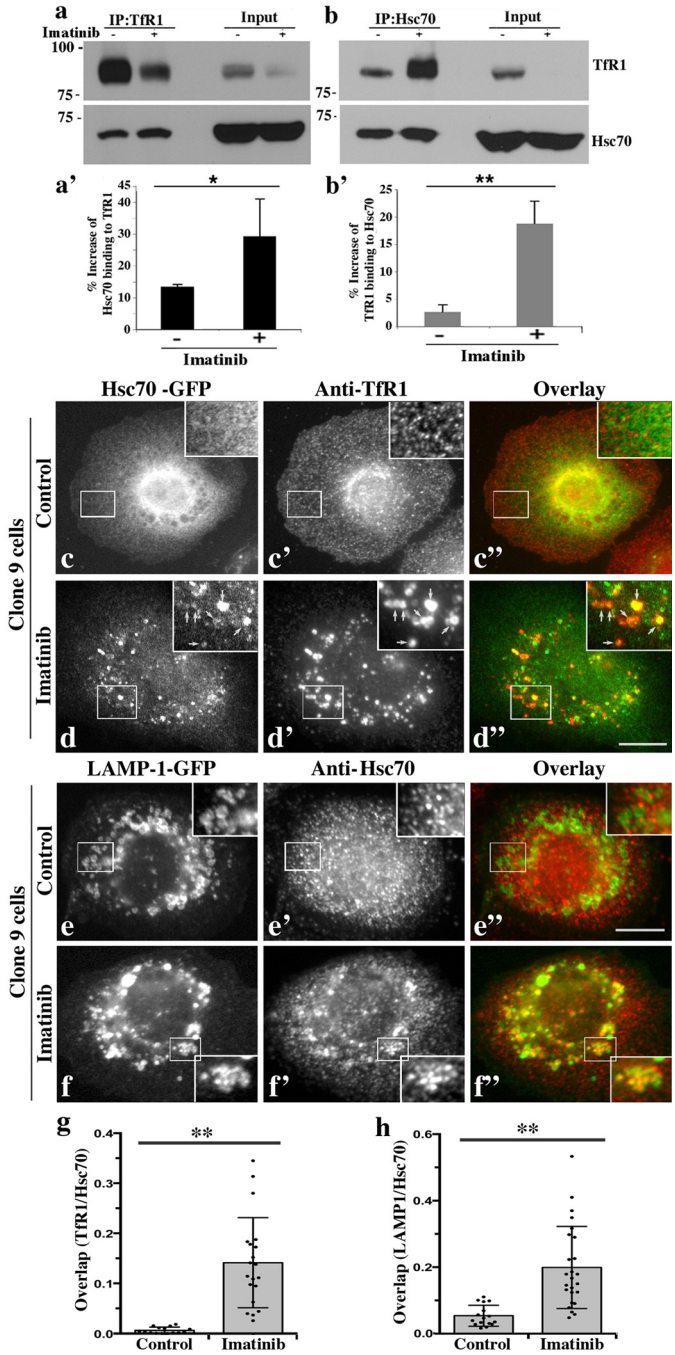

FIGURE 8. **TfR1 association with the chaperone Hsc70 increases upon c-Abl inhibition by imatinib.** *a* and *b*, following imatinib treatment, clone 9 cells were subjected to coimmunoprecipitation using an antibody against TfR1 (*a*) or Hsc70 (*b*) and analyzed by Western blot. Note that binding between the two proteins increased markedly after c-Abl inhibition. *a'* and *b'*, quantitation of three independent experiments as described in *a* and *b*. Data are presented as mean ± S.E.; **, $p < 0.01$. *c–f*, clone 9 cells expressing Hsc70-GFP or LAMP1-GFP were treated with vehicle control (*c* and *e*) or 20 μg/ml imatinib (*d* and *f*) for 2 h and subsequently analyzed by immunofluorescence microscopy using an antibody against TfR1 (*c'* and *d'*) or LAMP1 (*e'* and *f'*) to assess colocalization between the proteins tested. Indeed, Hsc70 colocalized with TfR1 and LAMP1 at the lysosome after imatinib treatment. *Scale bar*, 10 μm. *g*, quantitation of the morphology-based experiments shown in *c* and *d* showing a marked increase in overlap between Hsc70-GFP- and TfR1 antibody-stained compartments following control or imatinib treatments. (Control, 0.6 ± 0.006%, $n = 15$ cells; imatinib: 14.1 ± 0.09, $n = 20$ cells.) *h*, quantitation of the morphology-based experiments as described in *e* and *f* showing LAMP1-GFP- and anti-Hsc70-stained compartments following control or imatinib treatments. A substantial increase in localization of the chaperone to the lysosome compartment is observed. (Control, 5.4 ± 0.031%, $n = 16$ cells; imatinib, 19.9 ± 0.12, $n = 25$ cells.) **, $p < 0.01$.

alone (DMSO, Fig. 9, *e* and *e''*) or the Hsc70 inhibitor (Fig. 9, *f*, *f'*, *g*, and *g'*), then treated with imatinib for 2 h, and stained with Hsc70 and TfR1-N antibodies. Immunofluorescence microscopy shows the characteristic imatinib-induced redistribution of both the receptor and chaperone to a large punctate putative endolysosome compartment (Fig. 9, *f* and *f'*). This effect is blocked by treatment with VER155008, as the Hsc70 distribution remains diffuse, and the TfR1 resides in smaller more numerous puncta compared with untreated cells. Control experiments testing the effects of VER155008 on clathrin-based uptake and distribution were performed, as Hsc70 is known to participate in the uncoating of clathrin-coated vesicles. Hsc70 inhibition might be expected to prevent TfR1 internalization at the cell surface and thus indirectly reduce lysosomal degradation. At the acute time periods used in these studies, an expected accumulation of clathrin at the surface of clone 9 cells was observed, although TfR1 internalization appeared normal (data not shown).

As imatinib induces the co-trafficking of these proteins to the endolysosome (Fig. 6), we sought to define the vesicular compartment in which the TfR1 resides as a result of Hsc70 inhibition. Constitutive transport of TfR1 to the lysosome upon Hsc70 inhibition and dissociation would contradict a model that Hsc70 function is essential for aberrant TfR1 transport for degradation upon inhibition of c-Abl. Clone 9 cells were treated as described above and stained for the early endosome marker EEA1 (Fig. 9, *h–i''*; supplemental Fig. S5, *a–f''*). Importantly, cells treated with both imatinib and VER155008 revealed a marked increase of TfR1 in EEA1-positive vesicles (Fig. 9, *i–i''*) and a great reduction in transit to the late endosome and lysosome (Fig. 9, *k* and *l*; supplemental Fig. S5, *a–f''*), suggesting that Hsc70 inhibition attenuated the transport of the receptor from the early endosome to the late endosome, perhaps by preventing the physical interaction between the chaperone and receptor cargo (Fig. 9, *c* and *d*).

Additional biochemical experiments were performed to support the VER155008 findings using a second Hsc70 inhibitor, 2-phenylethyne sulfonamide (PES). This compound affects all Hsc/Hsp family members through a non-specific detergent-like interaction with the substrate binding domain of these proteins (33). We pretreated clone 9 cells with PES (25 μM) for 2 h and then added 20 μg/ml imatinib for 2 h before lysis and Western blotting analysis (supplemental Fig. S4). Cells treated with vehicle alone (DMSO) exhibited the characteristic stepwise reduction of TfR1 levels. As expected, the PES-treated cells exhibited a marked protection of TfR1 total protein levels. Finally, as Hsc70 has been implicated in chaperone-mediated autophagy of proteins to the lysosome (34), we tested whether an siRNA knockdown of LAMP2a might protect the TfR1 from degradation in imatinib-treated cells. LAMP2a is known to provide a functional pore that mediates the transit of cargo proteins to be degraded from the cytoplasm to the lysosomal lumen (34). As depicted in Fig. 9, *m* and *n*, a near complete siRNA-based reduction of the LAMP2a protein had no effect

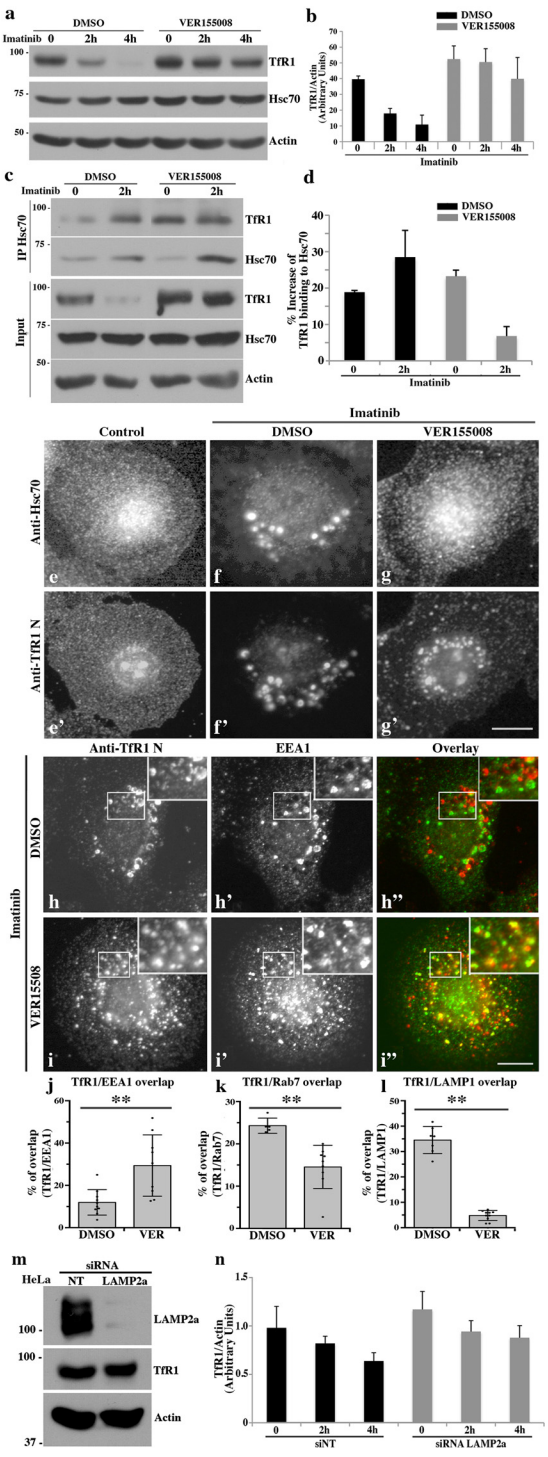

FIGURE 9. **Hsc70 inhibition substantially reduces TfR1 degradation in imatinib-treated cells.** *a* and *b*, Western blotting analysis and corresponding quantitation (three experiments) of TfR1 levels in clone 9 cells pretreated with DMSO or the Hsc70 inhibitor VER155008 (100 μM) for 16 h and then treated with 20 μg/ml imatinib over different time periods (0, 2, and 4 h). Inhibition of Hsc70 function by VER155008 prevented the loss of the TfR1. Data are presented as mean ± S.E. **, $p < 0.01$. *c* and *d*, Western blotting analysis and corresponding quantitation (three experiments) measuring the interactions between TfR1 and Hsc70 in response to VER155008. Data are presented as mean ± S.E. **, $p < 0.01$. Cells were treated as described above but subjected to an immunoprecipitation of Hsc70 prior to SDS-PAGE and Western blot. Total protein shown in the input lanes again reveal a protection of the TfR1 by VER155008 drug as in *a* and *b*. A significantly reduced association is observed when Hsc70 function is inhibited despite the fact that the levels of this protein are increased. *e* and *e'* and *g* and *g'*, immunofluorescence images of Hsc70 and TfR1 in clone 9 cells pretreated with DMSO (*e* and *e'*) or the Hsc70 inhibitor overnight (*f*, *f'* and *g* and *g'*) and then treated with imatinib for 2 h. Imatinib induces the redistribution of both the receptor and chaperone to large punctate, putative endolysosome compartments (*f* and *f'*) that is blocked by treatment with VER155008. *h–i''*, immunofluorescence images of EEA1 and TfR1 in clone 9 cells treated as above show a retention of the receptor in the early endosome in Hsc70 inhibited cells. *j–l*, quantitative analysis of the changes in TfR1 distribution in imatinib-treated clone 9 cells following treatment with DMSO or VER155008 (100 μM) for 10 h. Although the overlap between the TfR1 compartments and the early endosome (EEA1) is substantially increased (*j*), trafficking to the late endosome (Rab7) or lysosome (LAMP1) is markedly reduced by inhibition of Hsc70 (*k* and *l*). Cell count numbers are as follows: *j*, DMSO, 12.0 ± 0.06%, $n = 10$ cells; VER155008, 29.4 ± 0.15%, $n = 9$ cells; *k*, DMSO, 24.3 ± 0.02%, $n = 5$ cells; VER155008, 14.5 ± 0.05%, $n = 9$ cells; and *l*, DMSO, 34.5 ± 0.05, $n = 7$ cells; VER155008, 5.0 ± 0.02%, $n = 12$ cells. **, $p < 0.01$. *Scale bars*, 10 μm. *m* and *n*, siRNA knockdown of the lysosome-associated membrane protein (LAMP2a) in HeLa cells over 3 days followed by SDS-PAGE and Western blotting analysis (*m*) results in a near complete reduction of the protein. *Graph* depicting three distinct experiments in which these cells were then treated with imatinib for 0, 2, and 4 h followed by Western blotting analysis of TfR1 levels. Little to no change in receptor levels is observed.

on the imatinib-based loss of the TfR1 suggesting that this is not a traditional chaperone-mediated autophagy pathway.

Discussion

TfR1 endocytosis and trafficking is generally cited as a "classic" constitutive pathway in which iron-bound transferrin and the associated receptor are internalized continuously and transported to an early recycling endosome, upon which the iron is dissociated by the acidic environment and the receptor-transferrin complex is transported back to the plasma membrane for reuse (6, 7). Based on our previous observations that Src kinase can regulate internalization and release of TfR1 containing clathrin-coated pits by tyrosine phosphorylation of Dyn2 and its actin binding partner cortactin (10, 11), it is possible that several potential layers of regulation exist that mediate the internalization and trafficking of this trophic receptor.

Our initial findings that internalization of the TfR1 is markedly reduced by pharmacological inhibition of c-Abl by imatinib (Fig. 1, *c* and *d*) was consistent with past reports by others that this kinase regulates the endocytosis of several different RTKs. These include antigen-receptor complexes in B lymphocytes via CrkII, Rac activation (35), and alterations in EGFR endocytosis (36). The initial surprise from this study was that imatinib appeared to alter the internalization of trophic receptors (Figs. 4*b* and 6, *d*, and *f*; supplemental Fig. S1) that exhibit minimal post-translational modifications, unlike the receptor systems cited above. Furthermore, inhibiting c-Abl function resulted in a drastic loss of the TfR1 from the cell surface (Fig. 4, *b* and *c*), hence explaining the reduced Tf uptake as an indirect but perhaps more interesting consequence of c-Abl inhibition. Relevant findings to this study are those of Pendergast and coworkers(36), who have observed significant effects on EGFR trafficking by altering c-Abl activity. In contrast to our findings with the TfR1, they have reported an "uncoupling" of the EGFR from ligand-mediated internalization in cells expressing active c-Abl as well as preventing the recruitment of the ubiquitin-ligase Cbl to the activated EGFR. Thus, activated c-Abl kinase results in the retention of this receptor on the cell surface for continued signaling, although attenuation of the kinase promotes its lysosomal trafficking (36). In contrast, we find that

overexpression of WT c-Abl kinase has little effect on Tf internalization, although inhibition of the kinase promotes receptor degradation (Figs. 2*b*′; 6, *a* and *b*, and 7, *a* and *b*; supplemental Fig. S2).

In addition to a reduction in EGFR internalization by active c-Abl, Pendergast and colleagues (37) also report that inhibition of c-Abl attenuates the trafficking and function of lysosomal components to the autophagosome, specifically the M6PR-mediated transport of glycosidases and cathepsins. Although lysosome-autophagosome fusion appears normal, c-Abl inhibition leads to an altered distibution and morphology. We have also observed morphological alterations in these organelles upon inhibition of c-Abl, although they remain competent to degrade the TfR1 and LDLR just over several hours, a process that is markedly reduced by lysosome inhibitors (Figs. 7, *a* and *b*; supplemental Fig. S3, *a* and *b*).

These observations indicated that c-Abl kinase may control the endocytic fate of the TfR1. Inhibition of this kinase diverts the internalized ligand-TfR1 complex away from the perinuclear Rab11 recycling endosome to the lysosome (Fig. 6, *g*–*h*″). This putative regulation is particularly interesting in the context of active *versus* default cargo sorting. The distinct endocytic fates of the two related TfRs make this regulation even more relevant. As mentioned, the TfR1 is recycled post-internalization, although the TfR2 is targeted for degradation into MVBs and subsequently to the lysosome. It remains unclear how the trafficking machinery discriminates between these two receptors and controls their intracellular trafficking, although one would predict that the 61-residue cytoplasmic tail is key.

It has been thought for some time that other than a canonical AP2-binding motif (*YXX*Φ), the TfR1 tail possessed little information that could direct its recycling back to the plasma membrane, suggesting this is a default pathway. Subsequently, several insightful studies have provided information as to how this internalized receptor can be directed back to the plasma membrane, and how c-Abl might participate in this process. First, the small regulatory GTPase Rab12 has been found to localize to the TfR1 recycling endosome in cells where its activity appears to direct the receptor to the lysosome for degradation (38). It is possible that c-Abl kinase could regulate this Rab either directly or through modification of a GTPase-activating protein of the guanine nucleotide exchange factor. Second, c-Abl has been shown to promote the autophagic process indirectly though activation of lysosome motility and capacity of lysosomes to degrade substrate (37). How imatinib facilitates TfR1-Hsc70 interaction and trafficking to the lysosome for degradation is unclear. Perhaps most relevant is the well documented identification of two distinct phenylalanine-based sequences in the cytoplasmic TfR1 tail that recruits the ARF6 GTPase-activating protein called ACAP1 (39). Importantly, this interaction appears to promote cargo sorting of GLUT4 as well as both TfR1 and the integrin receptors (6). It is attractive to predict that c-Abl activity could alter the TfR1 tail-ACAP1 interaction to regulate the recycle-degrade switch of this receptor.

Ubiquitylation of internalized RTKs (40) provides another well defined targeting motif recognized by the ESCRT machinery for transport to the MVB and subsequent degradation (41). Whether inhibition of c-Abl kinase potentiates this ubiquitin modification is unclear. We have conducted some additional control experiments testing for ubiquitylation of this receptor and the EGFR as a control in either Hep3b or clone 9 cells that were then treated with bafilomycin to promote the accumulation of any ubiquitylated protein targeted to the lysosome. We did observe a consistent modification of the EGFR, but not the TfR1 (data not shown), suggesting that TfR1 may not be subjected to ubiquitin-based targeting. It should be noted, however, that one study has shown extensive evidence that an excess of iron added to cultured cells results in a ubiquitylation of the TfR1 leading to lysosomal targeting (27). More recently, the same group (42) has reported that several lysines on the cytoplasmic tail of this receptor in COS7 cells are modified by a RING-type ubiquitin-ligase (MARCH8). This specific ubiquitylation event leads to the predicted degradation-based down-regulation of the TfR1. Whether this iron-induced response is distinct to the c-Abl-mediated degradation is unclear.

Because lysosomal degradation of target proteins can occur through Ub-independent pathways, we tested whether imatinib-induced TfR1 degradation involved the ESCRT complex, which targets its cargo through the MVB to the lysosome (43). Accordingly, we reduced the cellular levels of the ubiquitin-binding ESCRT1 member Tsg101 by siRNA treatment to test whether this might prevent the imatinib-induced loss of either the TfR1 or the EGFR as a control (Fig. 7, *e*–*g*). Importantly, the reduction of Tsg101 prevented the degradation of both receptors suggesting that the imatinib-induced degradative pathway of the TfR1 is mediated by ESCRT function.

Although all of the processes described above provide plausible mechanisms for how c-Abl activity might support TfR1 recycling back to the cell surface, we focused our attention on the action of the cytoplasmic chaperone Hsc70, well known to mediate a diverse set of cellular functions that include the uncoating of clathrin vesicles (44–46), facilitating appropriate protein folding (47), and directing cellular organelles into the autophagic pathway (48, 49), to name just a few. The interactions between this chaperone and the TfR1 upon inhibition of c-Abl by imatinib as assessed by co-IP (Fig. 7, *a* and *b*) were pronounced and further supported by graphic changes in the Hsc70 distribution from cytosolic to a more punctate vesicular localization (Fig. 7*c*). Importantly, we found that these structures represent LAMP1-positive compartments containing the TfR1. From previous studies by others, it is known that Hsc70 interacts with the tail region of TfR1 in exosomes (50, 51). Also, Hsc70 is known to interact with the cytosolic domain of the TfR1 through the ^{20}YTRFSLARQV^{29} (amino acids 20–29 in TfR1) (52). It is well documented that Hsc70 mediates transport of proteins and organelles to autophagosomes via interaction with target proteins containing a KFERQ motif (53, 54) that can vary considerably in primary sequence. It is particularly attractive to speculate that the cytoplasmic tail of the TfR1 might contain a KFERQ motif that could then facilitate targeting to the lysosome via an Hsc70 interaction. We have not observed any direct interactions between the chaperone and receptor. Moreover, although our sequence analysis identified a putative Hsc70-binding motif in the TfR1 tail (^{23}FSLARQV^{29}) that possessed some similarity to the Hsc70-binding region in the EGFR

(29, 36), mutation or deletion of this motif had no effect on imatinib-induced trafficking to the lysosome. This was tested in clone 9 cells, fibroblasts, and a CHO cell line devoid of native TfR1 (data not shown) (55).

In addition to the dramatic recruitment of Hsc70 to the TfR1 endosomes upon inhibition of c-Abl, we have observed a substantial "protection" of this receptor from degradation through drug-based inhibition of the chaperone. The prevalence of these chaperones makes it difficult to inhibit their function by siRNA knockdown or mutant protein expression. Therefore, this was performed with two widely used inhibitors as follows: VER155008, which binds to the ATPase domain of Hsc70; and PES, which inhibits most Hsc/Hsp family members through a non-specific detergent-like interaction with the substrate binding domain of these proteins (Figs. 9, *a* and *b*; supplemental Fig. S4). These experiments provide some functional insights, coupled with the biochemical and morphological findings, into the requirement of the Hsc70 chaperone for receptor trafficking and subsequent degradation. Equally important is the fact that in imatinib-treated cells, Hsc70 inhibition causes an increase of TfR1 in EEA1-positive early endosomes (Fig. 9, *i* and *j*), as viewed by IF, although much less TfR1 reaches the late endosome/lysosome (Figs. 9, *k* and *l*; supplemental Fig. S5, *a–f′*), suggesting that c-Abl mediates the chaperone-based transport event between the early and late endosomes. This process does not appear to be dependent upon LAMP2a, known to mediate the transfer of degraded cargo from the cytoplasm to the lysosomal lumen during chaperone-mediated autophagy as siRNA-based reduction of this glycoprotein did not change TfR1 levels (Fig. 9, *m* and *n*). Future studies will continue to focus on defining the exact mechanisms by which this important family of kinases and chaperones might interact to regulate receptor trafficking in epithelial cells.

Experimental Procedures

Miniprep express matrix and Luria-Bertani medium were from BIO 101 (Vista, CA). Plasmid purification and gel extraction kits were purchased from Qiagen (Alameda, CA). Restriction enzymes were purchased from New England Biolabs (Ipswich, MA). 1-kb plus DNA ladder was from Life Technologies, Inc.. c-Abl and EEA1 monoclonal antibodies were from Pharmingen, and anti-TfR1 monoclonal antibody was from Zymed Laboratories Inc.. LAMP1 (C-20) and anti-Hsc70 (B-6) monoclonal antibodies were purchased from Santa Cruz Biotechnology (Dallas, TX); anti-LAMP2a polyclonal antibody was purchased from Abcam (Cambridge, MA) and anti-TSG101 monoclonal antibody was purchased from GeneTex (Irvine, CA). The rabbit polyclonal anti-TfR1 antibody was raised by our laboratory as described previously (11). The rabbit polyclonal anti-LDLR1 was raised against the peptide PVYQKTTEDEIHICRSQDGYTYPS, present in the C-terminal region of LDLR. An anti-actin antibody was purchased from Sigma. Goat anti-rabbit and goat anti-mouse secondary antibodies conjugated to either Alexa-Fluor-488 or -594. Transferrin Alexa-Fluor-488 and -594 and rhodamine- and FITC-dextran (M_r 3,000) used for immunofluorescent staining were all obtained from Life Technologies, Inc., and HRP-conjugated goat anti-rabbit and goat anti-mouse were from BioSource International, Inc. (Camarillo, CA), which were used for Western blotting analysis. LysoTracker Deep Red was purchased from Invitrogen. c-Abl inhibitor Imatinib (Gleevec) was purchased from Cayman Chemical (Ann Arbor, MI). The lysosomal inhibitor bafilomycin A1 was purchased from Enzo Life Sciences (Farmingdale, NY). The Hsc70 inhibitors VER155008 and Pifithrin-μ (PES) and all other chemicals and reagents, unless otherwise stated, were from Sigma.

Plasmid Construction—The GFP-tagged TfR1 construct was generated as described previously (11). The untagged c-Abl WT was designed using an oligonucleotide primer specific for c-Abl-1a and -1b according to the rat c-Abl-1a and -1b sequences from GenBank™ (accession numbers XM_006233918 and NM_001100850) as follows: c-Abl-1a, 5′-CGCCGTGGCCACGGGACCATGTTGGAGA; c-Abl-1b, 5′-ATGGGGCAGCAGCCTGGAAAAGTACTTGGG; and c-Abl-1, 3′-CTACCTCCGGACAATGTCGCTGATCTCCTT. Full-length cDNA was amplified by long distance reverse transcription-PCR (RT-PCR; Applied Biosystems, Branchburg, NJ), and the PCR fragments were ligated into the eukaryotic expression vector pCR3.1 (Invitrogen). Kinase-dead c-Abl-1a K266R, inactive c-Abl-1a Y412F, kinase-dead c-Abl-1b K290R, and inactive c-Abl-1b Y437F mutants were generated using PCR-based mutagenesis methods. The GFP-tagged Hsc70 WT was designed using an oligonucleotide primer specific for Hsc70 according to the rat Hsc70 sequence from GenBank™ (accession numbers NM_024351 and XM_001053026) as follows: Hsc70, 5′-CTCGAGTGGGCCTACACGCAAGCAACCAT, and Hsc70, 3′-GAATTCCCTCTACTTTGACGTAATCGACC. Full-length Hsc70 cDNA was amplified by long distance (RT-PCR), and the end product was ligated into pEGFP-N1 (Clontech). The GFP-tagged LAMP1 WT was designed using oligonucleotide primers specific for LAMP1 according to the rat LAMP1 sequence from GenBank™ (accession numbers NM_012857) as follows: LAMP1, 5′-GATCGAATTCCAACCGCCGTCCTTCGGCCTC; LAMP1, 3′-GATCGGATCCCGCACCTGCCCACCAGGCAAGATG. Full-length LAMP1 cDNA was amplified by long distance (RT-PCR) using rat liver cDNA, and the end product was ligated into pEGFP-N1 (Clontech). All DNA constructs were verified by restriction enzyme digestion and sequence analysis. All plasmids were purified either by equilibrium centrifugation in a CsCl-ethidium bromide gradient or with the plasmid maxi kit from Qiagen.

siRNA Oligonucleotides—Non-targeting siRNA and all targeting siRNAs were from Dharmacon (GE Healthcare) as follows: human LAMP2a, 5′-GGCAGGAGUACUUAUUCUAUU-3′; and TSG101, 5′-CCUCCAGUCUUCUCUCGU C-3′. The oligonucleotides were received in an annealed and purified form ready to be transfected upon resuspension in Opti-MEM I (Gibco).

Cell Culture and Transfection—Clone 9 rat hepatocytes were incubated in F12K medium supplemented with 10% FBS and 50 units/mg penicillin + 50 μg/ml streptomycin. HeLa cells were propagated in minimum Eagle's medium + 10% FBS and 50 units/mg penicillin + 50 μg/ml streptomycin. Hep3b human hepatocellular carcinoma cells from ATCC (HB-8064) were incubated in MEM supplemented with 10% FBS and 50 units/mg penicillin + 50 μg/ml streptomycin. MEFs, c-Abl$^{-/-}$,

and c-Abl/Arg$^{-/-}$ MEFs were a kind of gift from Dr. A. Pendergast (Duke University, Durham, NC) and were maintained in DMEM + 10% FBS and 50 units/mg penicillin + 50 μg/ml streptomycin. All cells were maintained at 5% CO_2, 95% air at 37 °C. Cells were transfected using Lipofectamine 2000 (Invitrogen) according to the manufacturer's instructions.

Assays for Internalization of Dextran and Transferrin, Pulse Labeling of Late Endosomal Compartments—Endocytosis of fluorescently conjugated transferrin or dextran was assayed as described previously (56).

Statistical Analysis—Statistical analysis was performed using a two-tailed Student's *t* test for each sample group. *p* values $\leq$ 0.05 were considered statistically significant and are indicated in each figure.

Immunofluorescence and IF-based Quantitation—Immunofluorescence staining was performed as described previously (57). Fluorescence micrographs were acquired using a Zeiss Axiovert 35 epifluorescence microscope (Carl Zeiss) equipped with a Hamamatsu Orca II camera (Hamamatsu Photonics, Hamamatsu City, Japan), and images were processed using Adobe Photoshop (Adobe). For IF-based quantification Tf internalization, all images were taken at the same exposure time and analyzed using IPLab software.

Surface Biotinylation Assay—Clone 9 cells were treated with 20 μg/ml imatinib for 0, 30, 60, or 120 min, then transferred to 4 °C, rinsed with chilled PBS, and incubated with 0.5 mg/ml biotin (EZ-link® Sulfo-NHS-LC Biotin, Thermo Scientific) for 30 min. Subsequently, biotin was quenched with 50 mM NH_4Cl, and cells were rinsed three times with PBS, lysed in RIPA buffer (150 mM NaCl, 1% Nonidet P-40, 0.5% sodium deoxycholate, 0.1% SDS, 50 mM Tris, pH 8), sonicated and centrifuged for 10 min, 14,000 rpm at 4 °C. Equal amounts of protein were added to 5 μg of TfR1 antibody and incubated for 2 h. Antibody-bound complexes were precipitated by adding protein A-coated beads (Sigma) for 1 h at 4 °C, washed five times with lysis buffer, and subjected to Western blotting analysis, together with ~10% of the input to determine the total amount of receptor in each sample.

Coimmunoprecipitation—HeLa or clone 9 cells were plated in 100-mm Petri dishes and grown to 70–90% confluence. The cells were treated for 2 h with 20 μg/ml imatinib or vehicle control before collecting cell lysates in hypotonic lysis buffer (10 mM Hepes, pH 7.5, 10 mM NaCl, 1 mM KH_2PO_4, 5 mM $NaHCO_3$, 1 mM $CaCl_2$, 0.5 mM $MgCl_2$, 5 mM EDTA, 10 mM sodium pyrophosphate, 1 mM Na_3VO_4, protease inhibitors). Subsequently, lysates were sonicated and centrifuged for 10 min, 14,000 rpm at 4 °C. 500–800 μg of lysate were added to 5 μg of antibody and incubated for 2 h at 4 °C. Antibody-bound complexes were precipitated by adding protein A- or G-coated beads (Sigma and Santa Cruz Biotechnology, respectively) for 1 h at 4 °C, washed five times, and subjected to Western blotting analysis.

Colocalization Quantitation—To quantify the colocalization between TfR1 with Hsc70-GFP, LAMP1-GFP, or Rab7-GFP or to quantify colocalization of Hsc70 with LAMP1-GFP, images were analyzed in ImageJ using the JACoP plugin (58). Using an objects-based method, the percentage overlap was calculated between particles (between 1 and 500 px^2) thresholded from each channel.

Author Contributions—B. S., H. C., and M. A. M. wrote the paper. H. C. designed, performed molecular biology, cell culture, and morphological analysis, and analyzed the experiments. J. C. performed all biochemistry work and analyzed the experiments. M. B. S. performed quantitation and analyzed the experiments shown in Fig. 8, *g* and *h,* and Fig. 9, *j–l.* All authors reviewed the results and approved the final version of the manuscript.

Acknowledgments—We thank the members of the McNiven laboratory for helpful discussions and Mary Schulz for critical reading of the manuscript.

References

1. Kawabata, H., Yang, R., Hirama, T., Vuong, P. T., Kawano, S., Gombart, A. F., and Koeffler, H. P. (1999) Molecular cloning of transferrin receptor 2. A new member of the transferrin receptor-like family. *J. Biol. Chem.* **274,** 20826–20832
2. Hopkins, C. R., and Trowbridge, I. S. (1983) Internalization and processing of transferrin and the transferrin receptor in human carcinoma A431 cells. *J. Cell Biol.* **97,** 508–521
3. Hentze, M. W., Muckenthaler, M. U., and Andrews, N. C. (2004) Balancing acts: molecular control of mammalian iron metabolism. *Cell* **117,** 285–297
4. Trinder, D., and Baker, E. (2003) Transferrin receptor 2: a new molecule in iron metabolism. *Int. J. Biochem. Cell Biol.* **35,** 292–296
5. Barisani, D., and Conte, D. (2002) Transferrin receptor 1 (TfR1) and putative stimulator of Fe transport (SFT) expression in iron deficiency and overload: an overview. *Blood Cells Mol. Dis.* **29,** 498–505
6. Hsu, V. W., Bai, M., and Li, J. (2012) Getting active: protein sorting in endocytic recycling. *Nat. Rev. Mol. Cell Biol.* **13,** 323–328
7. De Domenico, I., McVey Ward, D., and Kaplan, J. (2008) Regulation of iron acquisition and storage: consequences for iron-linked disorders. *Nat. Rev. Mol. Cell Biol.* **9,** 72–81
8. Johnson, M. B., Chen, J., Murchison, N., Green, F. A., and Enns, C. A. (2007) Transferrin receptor 2: evidence for ligand-induced stabilization and redirection to a recycling pathway. *Mol. Biol. Cell* **18,** 743–754
9. Chen, J., Wang, J., Meyers, K. R., and Enns, C. A. (2009) Transferrin-directed internalization and cycling of transferrin receptor 2. *Traffic* **10,** 1488–1501
10. Zhu, J., Yu, D., Zeng, X. C., Zhou, K., and Zhan, X. (2007) Receptor-mediated endocytosis involves tyrosine phosphorylation of cortactin. *J. Biol. Chem.* **282,** 16086–16094
11. Cao, H., Chen, J., Krueger, E. W., and McNiven, M. A. (2010) SRC-mediated phosphorylation of dynamin and cortactin regulates the "constitutive" endocytosis of transferrin. *Mol. Cell. Biol.* **30,** 781–792
12. Cao, H., Garcia, F., and McNiven, M. A. (1998) Differential distribution of dynamin isoforms in mammalian cells. *Mol. Biol. Cell* **9,** 2595–2609
13. Cao, H., Orth, J. D., Chen, J., Weller, S. G., Heuser, J. E., and McNiven, M. A. (2003) Cortactin is a component of clathrin-coated pits and participates in receptor-mediated endocytosis. *Mol. Cell. Biol.* **23,** 2162–2170
14. McNiven, M. A. (1998) Dynamin: a molecular motor with pinchase action. *Cell* **94,** 151–154
15. McNiven, M. A., Kim, L., Krueger, E. W., Orth, J. D., Cao, H., and Wong, T. W. (2000) Regulated interactions between dynamin and the actin-binding protein cortactin modulate cell shape. *J. Cell Biol.* **151,** 187–198
16. Orth, J. D., and McNiven, M. A. (2003) Dynamin at the actin-membrane interface. *Curr. Opin. Cell Biol.* **15,** 31–39
17. Buchdunger, E., O'Reilly, T., and Wood, J. (2002) Pharmacology of imatinib (STI571). *Eur. J. Cancer* **38,** Suppl. 5, S28–S36
18. Manley, P. W., Cowan-Jacob, S. W., Buchdunger, E., Fabbro, D., Fendrich, G., Furet, P., Meyer, T., and Zimmermann, J. (2002) Imatinib: a selective tyrosine kinase inhibitor. *Eur. J. Cancer* **38,** Suppl. 5, S19–27

19. Lin, Y. L., Meng, Y., Jiang, W., and Roux, B. (2013) Explaining why Gleevec is a specific and potent inhibitor of Abl kinase. *Proc. Natl. Acad. Sci. U.S.A.* **110,** 1664–1669
20. Druker, B. J., Tamura, S., Buchdunger, E., Ohno, S., Segal, G. M., Fanning, S., Zimmermann, J., and Lydon, N. B. (1996) Effects of a selective inhibitor of the Abl tyrosine kinase on the growth of Bcr-Abl positive cells. *Nat. Med.* **2,** 561–566
21. O'Dwyer, M. E., and Druker, B. J. (2000) Status of bcr-abl tyrosine kinase inhibitors in chronic myelogenous leukemia. *Curr. Opin. Oncol.* **12,** 594–597
22. Theis, S., and Roemer, K. (1998) c-Abl tyrosine kinase can mediate tumor cell apoptosis independently of the Rb and p53 tumor suppressors. *Oncogene* **17,** 557–564
23. Srinivasan, D., Kaetzel, D. M., and Plattner, R. (2009) Reciprocal regulation of Abl and receptor tyrosine kinases. *Cell. Signal.* **21,** 1143–1150
24. Hantschel, O., and Superti-Furga, G. (2004) Regulation of the c-Abl and Bcr-Abl tyrosine kinases. *Nat. Rev. Mol. Cell Biol.* **5,** 33–44
25. Bradley, W. D., and Koleske, A. J. (2009) Regulation of cell migration and morphogenesis by Abl-family kinases: emerging mechanisms and physiological contexts. *J. Cell Sci.* **122,** 3441–3454
26. Lagace, T. A. (2014) PCSK9 and LDLR degradation: regulatory mechanisms in circulation and in cells. *Curr. Opin. Lipidology* **25,** 387–393
27. Tachiyama, R., Ishikawa, D., Matsumoto, M., Nakayama, K. I., Yoshimori, T., Yokota, S., Himeno, M., Tanaka, Y., and Fujita, H. (2011) Proteome of ubiquitin/MVB pathway: possible involvement of iron-induced ubiquitylation of transferrin receptor in lysosomal degradation. *Genes Cells* **16,** 448–466
28. Raiborg, C., and Stenmark, H. (2009) The ESCRT machinery in endosomal sorting of ubiquitylated membrane proteins. *Nature* **458,** 445–452
29. Shen, S., Zhang, P., Lovchik, M. A., Li, Y., Tang, L., Chen, Z., Zeng, R., Ma, D., Yuan, J., and Yu, Q. (2009) Cyclodepsipeptide toxin promotes the degradation of Hsp90 client proteins through chaperone-mediated autophagy. *J. Cell Biol.* **185,** 629–639
30. Beau, I., and Codogno, P. (2010) GTP: gatekeeper for autophagy. *Mol. Cell* **39,** 485–486
31. Wirawan, E., Vanden Berghe, T., Lippens, S., Agostinis, P., and Vandenabeele, P. (2012) Autophagy: for better or for worse. *Cell Res.* **22,** 43–61
32. Schlecht, R., Scholz, S. R., Dahmen, H., Wegener, A., Sirrenberg, C., Musil, D., Bomke, J., Eggenweiler, H. M., Mayer, M. P., and Bukau, B. (2013) Functional analysis of Hsp70 inhibitors. *PLoS One* **8,** e78443
33. Leu, J. I., Pimkina, J., Pandey, P., Murphy, M. E., and George, D. L. (2011) HSP70 inhibition by the small-molecule 2-phenylethynesulfonamide impairs protein clearance pathways in tumor cells. *Mol. Cancer Res.* **9,** 936–947
34. Cuervo, A. M., and Wong, E. (2014) Chaperone-mediated autophagy: roles in disease and aging. *Cell Res.* **24,** 92–104
35. Jacob, M., Todd, L. A., Majumdar, R. S., Li, Y., Yamamoto, K., and Puré, E. (2009) Endogenous cAbl regulates receptor endocytosis. *Cell. Signal.* **21,** 1308–1316
36. Tanos, B., and Pendergast, A. M. (2006) Abl tyrosine kinase regulates endocytosis of the epidermal growth factor receptor. *J. Biol. Chem.* **281,** 32714–32723
37. Yogalingam, G., and Pendergast, A. M. (2008) Abl kinases regulate autophagy by promoting the trafficking and function of lysosomal components. *J. Biol. Chem.* **283,** 35941–35953
38. Matsui, T., Itoh, T., and Fukuda, M. (2011) Small GTPase Rab12 regulates constitutive degradation of transferrin receptor. *Traffic* **12,** 1432–1443
39. Dai, J., Li, J., Bos, E., Porcionatto, M., Premont, R. T., Bourgoin, S., Peters, P. J., and Hsu, V. W. (2004) ACAP1 promotes endocytic recycling by recognizing recycling sorting signals. *Dev. Cell* **7,** 771–776
40. Goh, L. K., and Sorkin, A. (2013) Endocytosis of receptor tyrosine kinases. *Cold Spring Harbor Perspect. Biol.* **5,** a017459
41. Dores, M. R., Paing, M. M., Lin, H., Montagne, W. A., Marchese, A., and Trejo, J. (2012) AP-3 regulates PAR1 ubiquitin-independent MVB/lysosomal sorting via an ALIX-mediated pathway. *Mol. Biol. Cell* **23,** 3612–3623
42. Fujita, H., Iwabu, Y., Tokunaga, K., and Tanaka, Y. (2013) Membrane-associated RING-CH (MARCH) 8 mediates the ubiquitination and lysosomal degradation of the transferrin receptor. *J. Cell Sci.* **126,** 2798–2809
43. Fujita, H., Yamanaka, M., Imamura, K., Tanaka, Y., Nara, A., Yoshimori, T., Yokota, S., and Himeno, M. (2003) A dominant negative form of the AAA ATPase SKD1/VPS4 impairs membrane trafficking out of endosomal/lysosomal compartments: class E vps phenotype in mammalian cells. *J. Cell Sci.* **116,** 401–414
44. Ungewickell, E. (1985) The 70-kd mammalian heat shock proteins are structurally and functionally related to the uncoating protein that releases clathrin triskelia from coated vesicles. *EMBO J.* **4,** 3385–3391
45. Heuser, J., and Steer, C. J. (1989) Trimeric binding of the 70-kD uncoating ATPase to the vertices of clathrin triskelia: a candidate intermediate in the vesicle uncoating reaction. *J. Cell Biol.* **109,** 1457–1466
46. Eisenberg, E., and Greene, L. E. (2007) Multiple roles of auxilin and hsc70 in clathrin-mediated endocytosis. *Traffic* **8,** 640–646
47. Sharma, S. K., Christen, P., and Goloubinoff, P. (2009) Disaggregating chaperones: an unfolding story. *Curr. Protein Pept. Sci.* **10,** 432–446
48. Massey, A. C., Zhang, C., and Cuervo, A. M. (2006) Chaperone-mediated autophagy in aging and disease. *Curr. Top. Dev. Biol.* **73,** 205–235
49. Dice, J. F. (2007) Chaperone-mediated autophagy. *Autophagy* **3,** 295–299
50. Mathew, A., Bell, A., and Johnstone, R. M. (1995) Hsp-70 is closely associated with the transferrin receptor in exosomes from maturing reticulocytes. *Biochem. J.* **308,** 823–830
51. Géminard, C., Nault, F., Johnstone, R. M., and Vidal, M. (2001) Characteristics of the interaction between Hsc70 and the transferrin receptor in exosomes released during reticulocyte maturation. *J. Biol. Chem.* **276,** 9910–9916
52. Géminard, C., De Gassart, A., Blanc, L., and Vidal, M. (2004) Degradation of AP2 during reticulocyte maturation enhances binding of hsc70 and Alix to a common site on TFR for sorting into exosomes. *Traffic* **5,** 181–193
53. Fourie, A. M., Sambrook, J. F., and Gething, M. J. (1994) Common and divergent peptide binding specificities of hsp70 molecular chaperones. *J. Biol. Chem.* **269,** 30470–30478
54. Bonaldo, P., and Sandri, M. (2013) Cellular and molecular mechanisms of muscle atrophy. *Dis. Model Mech.* **6,** 25–39
55. McGraw, T. E., Greenfield, L., and Maxfield, F. R. (1987) Functional expression of the human transferrin receptor cDNA in Chinese hamster ovary cells deficient in endogenous transferrin receptor. *J. Cell Biol.* **105,** 207–214
56. Cao, H., Chen, J., Awoniyi, M., Henley, J. R., and McNiven, M. A. (2007) Dynamin 2 mediates fluid-phase micropinocytosis in epithelial cells. *J. Cell Sci.* **120,** 4167–4177
57. Henley, J. R., and McNiven, M. A. (1996) Association of a dynamin-like protein with the Golgi apparatus in mammalian cells. *J. Cell Biol.* **133,** 761–775
58. Bolte, S., and Cordelières, F. P. (2006) A guided tour into subcellular colocalization analysis in light microscopy. *J. Microsc.* **224,** 213–232